



# Modeling and analyzing the dynamics of brucellosis disease with vaccination in the fractional derivative under real cases

Bashir Al-Hdaibat<sup>1</sup> · Muhammad Altaf Khan<sup>2,3,4</sup> · Irfan Ahmad<sup>5</sup> · Ebraheem Alzahrani<sup>6</sup> · Ali Akgul<sup>7,8,9,10</sup>

Received: 12 February 2025 / Revised: 28 February 2025 / Accepted: 2 March 2025 /  
Published online: 21 March 2025  
© The Author(s) 2025

## Abstract

The present explores the brucellosis model in non-integer derivative by utilizing the real statistics from the mainland China. The formulation of the model first presented in integer order derivative and subsequently extended to fractional order using the Caputo derivative. The existence and uniqueness of the nonlinear fractional system is confirmed, which is the important requirement for a fractional nonlinear model. The local asymptotical stability of the fractional model when  $\mathcal{R}_0 < 1$  is analyzed. When  $\mathcal{R}_0 \leq 1$ , the model is found globally asymptotically stable. The existence of an endemic equilibria is given and found that the model has a unique endemic

---

✉ Muhammad Altaf Khan  
altafdir@gmail.com; muhammadaltafkhan@korea.ac.kr

- <sup>1</sup> Department of Mathematics, Faculty of Science, The Hashemite University, Zarqa, Jordan
- <sup>2</sup> School of Health and Environmental Science, Korea University, Seoul 02841, South Korea
- <sup>3</sup> Faculty of Natural and Agricultural Sciences, University of the Free State, Bloemfontein 9300, South Africa
- <sup>4</sup> Laboratory of Vaccine and Biomolecules, Institute of Bioscience, Universiti Putra Malaysia, UPM, 43400 Serdang, Selangor, Malaysia
- <sup>5</sup> Department of Clinical Laboratory Sciences, College of Applied Medical Science, King Khalid University, 61421 Abha, Saudi Arabia
- <sup>6</sup> Department of Mathematics, Faculty of Science, King Abdulaziz University, P.O. Box 80203, 21589 Jeddah, Saudi Arabia
- <sup>7</sup> Department of Electronics and Communication Engineering, Saveetha School of Engineering, SIMATS, Chennai, Tamilnadu, India
- <sup>8</sup> Department of Mathematics, Art and Science Faculty, Siirt University, 56100 Siirt, Turkey
- <sup>9</sup> Department of Computer Engineering, Biruni University, 34010 Topkapı, Istanbul, Turkey
- <sup>10</sup> Department of Mathematics, Mathematics Research Center, Near East University, 99138 Nicosia, Mersin 10, Turkey

equilibrium. Using the reported cases of brucellosis in mainland China from 2004 to 2018 are considered. Graphical results for data fitting in cumulative and daily wise are presented with their respective residuals. The basic reproduction number is obtained from data fitting is  $\mathcal{R}_0 = 1.0327$ . A numerical scheme for the Caputo case is provided in detailed and later the scheme was used to obtain the numerical results graphically. Various results regarding the disease curtail are presented graphically, that will be helpful for the disease elimination in the long run. The public health authority and the health agencies can utilize this work confidently for brucellosis control in mainland China.

**Keywords** Brucellosis vaccination system · China mainland data · Stability results · Estimations · Simulations

**MSC Codes:** 34A08 · 34D20 · 65L05

## 1 Introduction

One of the most common zoonotic illnesses worldwide is brucellosis, which is brought on by different strains of the *Brucella* virus. Sheep, cattle, pigs, and dogs can all harbor *Brucella*, one of the human-related viruses [1]. The livestock industry's profitability and human health are severely impacted by brucellosis [1, 2]. Around 500,000 new cases of brucellosis are reported each year in more than 160 countries worldwide [3, 4]. Animal and human brucellosis have been presented in China since the 20th century. In the 1950s and 1970s, things were bad. Throughout the 1980s, it steadily decreased, and by the 1990s, it was essentially under control. Following 2000, it saw a swift recovery until 2016 [3, 5]. Controlling brucellosis impact farmer's profit by affecting livestock breeding decisions. Profit depends on selling livestock, with prices influenced by supply and demand. When prices rise, farmers expand breeding, and when prices fall, they reduce it. Control measures, including disease management costs, affects profits, requiring farmers to adopt appropriate strategies to maximize earnings [6–8].

A mathematical model may theoretically examine the consequences of various control strategies in conjunction with observation data and clearly illustrate the epidemiological law of the disease [9–13]. Numerous researchers have conducted epidemiological studies on brucellosis using mathematical models. Through these investigations, they have discovered a number of significant factors. Two methods of brucellosis transmission in sheep were proposed by Ainseba et al. in 2010 [12]: the indirect transmission from environment and the direct transmission with infected individuals. In [14], the brucellosis disease model has been considered under the age of infection and waning immunity. The authors considered different routes of transmission and presented their model results. A deterministic model was put up by Li et al. [13], who came to the conclusion that testing, immunization, and mixed cross-infection are crucial elements. According to source [15], factors that include animal import, culling practices, and sterilization efforts are significant variables influencing brucellosis in Jilin province. Subsequent research revealed that brucellosis epidemics

had unique cyclical and seasonal reproduction mechanisms [16, 17]. In [18–21], they took into account the age structure and put forth a dynamical model with multi-stage pertaining to adult and young sheep. Numerous population dynamical models have characterized animal interactions, including mutual effect and infection between groups [22–24]. Various other approaches to handle the epidemic models have been considered in literature, see for example [25–27]. For instance, the neural network approach has been considered by the authors in [25] to solve the coronavirus disease model. The bayesian regularization method to solve the Layla and Majnun model constructed in fractional derivative has been investigated in [26]. The Bayesian regularization neural network to handle the chickenpox disease model numerically has been studied in [27].

In the literature, the mathematical models that are constructed in non-integer derivatives are regarded more reputable for a number of reasons, including crossover behaviors, memory effect, and hereditary features. It is also useful in epidemic model under real data, which were proven that the fractional models provide best fitting results. Due to the fractional order parameter, various possibilities for the model solution are exists and various results regarding the model are obtained. Various disease models for understanding infections diseases have been documented in the literature [28–31] that describe the benefits and characteristics of fractional order derivatives. For instance, the COVID-19 infection in fractional derivative using singular and non-singular kernel has been discussed in [28]. The Mittag-Leffler function's influence on the investigation of coronavirus infection was taken into account by the authors in [29]. The dynamical analysis of the Zika virus infection in non-integer derivative is discussed in [30]. They, then presented new mathematical and numerical conclusions along with a numerical technique for its solution numerically. In [31], the authors constructed a mathematical framework to analyze the Nipah virus dynamics. Their work introduced the concept of piece-wise fractional derivatives is an extension of traditional derivatives. This innovative approach allowed them to derive significant mathematical results associated to the system. The fractional order model was solved by the authors in [32] using a Simulink-based approach. In order to solve the infection system, [33] explored the concept of the fuzzy fractional derivative within the framework of the ABC derivative. The authors considered the fractional model with uncertainty using the predictive control has been studied in [34]. The work in [35] provides a recently developed system associated to the coronavirus with vaccination using fractional derivative concept. The concept of fractional derivative in terms of discrete case has been shown in [36] where the model of coronavirus was taken of coronavirus. The HIV dynamical model in fractional derivative has been considered in [37]. They considered in the modeling the operators Atangaa-Baleanu and Caputo Fabrizio derivative by presenting their results. In [38], the lymphatic disease model has been considered in fractional derivative. Mathematical interaction of the dynamics of Buruli ulcer in possum mammals in the framework of fractional derivative in [39]. In [40], they considered the avian spirochetosis model in non-singular and non-local kernels to understand their modeling and analysis.

This work aims to formulate a mathematical model in fractional derivative to analyze the brucellosis disease dynamics in the mainland China under the reported cases. The model initially formulated in classical derivative and then extended to fractional

derivative model. The model analysis has been analyzed for the fractional cases and then the estimation of parameters were obtained. Numerical results were obtained and discussed. Section-wise analysis of the work given in this paper is as follows: The modeling and of model under fractional calculus is given in Sect. 2. In Sect. 3, we provide the existence of fractional order system while Sect. 4 provides the equilibrium analysis. Parameter estimations and numerical scheme to solve fractional system have been discussed in Sects. 5 and 6 respectively. Sections 7 and 8 underscore the numerical simulation and conclusion.

## 2 Basic concepts associated to fractional calculus

Here, we shall provide some basic concepts regarding the fractional derivative in Caputo sense [41, 42].

**Definition 1** For a function  $k$ , the Caputo derivative of order  $\eta$  is defined by

$$D^\eta k(t) = \frac{1}{\Gamma(n-\eta)} \int_0^t (t-\tau)^{n-\eta-1} k^{(n)}(\tau) d\tau, \quad t > 0, \quad (1)$$

if  $\eta \notin \mathbb{N}$ ,  $n = [\eta] + 1$ . The following definition provided the fractional integral in Riemann-Liouville of the function  $k : \mathbb{R}^+ \rightarrow \mathbb{R}$ :

$$I^\eta k(t) = \frac{1}{\Gamma(\eta)} \int_0^t (t-\tau)^{\eta-1} k(\tau) d\tau. \quad (2)$$

### 2.1 Mathematical model

Modeling the brucellosis dynamics, we formula a mathematical model by the interaction of livestock and humans. Dividing the livestock into Susceptible livestock,  $S(t)$ , infected livestock,  $I(t)$ , and the vaccinated livestock,  $V(t)$ . The humans healthy and infected people are respectively given by  $S_h(t)$  and  $I_h(t)$ . The quantity of the brucellosis in the environment is shown by  $E(t)$ . Here,  $N_1$  and  $N_2$  are the total population of brucellosis and humans, which are respectively given by,  $N_1 = S + I + V$ , and  $N_2 = S_h + I_h$ . The recruitment rate of the livestock is  $\Lambda$ ,  $\kappa$  is the natural death rate of livestock in each compartment,  $\theta$  is the vaccination rate of healthy livestock, livestock lose of immunity rate  $\omega$ . The culling rate of infected livestock after being identified infected, at the rate of  $\mu$ . The transmission routes of brucellosis can be of with the infected livestock or with the pathogens in the environment. Here,  $\tau_1$  is the transmission of healthy and infected livestock, while the environmental transmission occur when the pathogens come in contact with the healthy livestock.  $\delta$  is the amount of discharged by the livestock in the environment, while  $\beta$  is the shedding rate of brucellosis in the environment. The birth rate of the humans population is given by  $\Lambda_h$ , while they die naturally at the rate  $\psi_h$ , the transmission routes are  $\phi_1$  and  $\phi_2$  which occur by the interaction of infected livestock with healthy humans, and the interaction of healthy humans with brucellosis in the environment. Humans are not transmitting

the brucellosis to other people, and not transmitting livestock. Usually, the healthy humans can be infected with the interaction of infected livestock or the brucellosis in the environment. Humans recovery rate is  $q$ . The above discussion leads to the following system of nonlinear evolutionary differential equations:

$$\begin{cases} \frac{dS}{dt} = \Lambda - \tau_1 \frac{SI}{N_1} - \tau_2 \frac{SE}{N_1} - \theta S + \omega V - \kappa S, \\ \frac{dV}{dt} = \theta S - \omega V - \kappa V, \\ \frac{dI}{dt} = \tau_1 \frac{SI}{N_1} + \tau_2 \frac{SE}{N_1} - \mu I - \kappa I, \\ \frac{dE}{dt} = \delta I - \beta E, \\ \frac{dS_h}{dt} = \Lambda_h - \phi_1 \frac{S_h I}{N_2} - \frac{\phi_2 S_h E}{N_2} - \psi_h S_h + q I_h, \\ \frac{dI_h}{dt} = \phi_1 \frac{S_h I}{N_2} + \frac{\phi_2 S_h E}{N_2} - \psi_h I_h - q I_h, \end{cases} \tag{3}$$

subject to initial conditions (ICs)

$$S(0) = S_0 > 0, \quad V(0) \geq V_0, \quad I_0 \geq I_0, \quad E_0 \geq 0, \quad S_h(0) > S_h(0), \quad I_h(0) \geq I_h(0). \tag{4}$$

If we look at the model (3), the last two equations are independent on the rest of equations, so, the dynamics of the model can be analyzed directly by the equations

$$\begin{cases} \frac{dS}{dt} = \Lambda - \tau_1 \frac{SI}{N_1} - \tau_2 \frac{SE}{N_1} - \theta S + \omega V - \kappa S, \\ \frac{dV}{dt} = \theta S - \omega V - \kappa V, \\ \frac{dI}{dt} = \tau_1 \frac{SI}{N_1} + \tau_2 \frac{SE}{N_1} - \mu I - \kappa I, \\ \frac{dE}{dt} = \delta I - \beta E. \end{cases} \tag{5}$$

### 2.2 Fractional model

We extend the model (5) into fractional order system by considering the Definition,

$$\begin{cases} D_t^\eta S = \Lambda - \tau_1 \frac{SI}{N_1} - \tau_2 \frac{SE}{N_1} - \theta S + \omega V - \kappa S, \\ D_t^\eta V = \theta S - \omega V - \kappa V, \\ D_t^\eta I = \tau_1 \frac{SI}{N_1} + \tau_2 \frac{SE}{N_1} - \mu I - \kappa I, \\ D_t^\eta E = \delta I - \beta E, \end{cases} \tag{6}$$

where  $D_t^\eta$  is the fractional derivative, and  $\eta \in (0, 1]$  is fractional order in Caputo sense.

### 3 Analysis of the fractional system

The analysis of the model (6) shall be carried out in the given section.

**Theorem 1** *All the solution of the fractional order brucellosis system (6) are nonnegative and bounded uniformly.*

**Proof** The following is obtained by following model (6):

$$\begin{aligned} D_t^\eta \Big|_{S=0} &= \Lambda + \omega V \geq 0, \\ D_t^\eta \Big|_{V=0} &= \theta S \geq 0, \\ D_t^\eta \Big|_{I=0} &= \tau_2 \frac{SE}{N_1 - I} \geq 0, \\ D_t^\eta \Big|_{E=0} &= \delta I \geq 0. \end{aligned} \quad (7)$$

Thus, it follows from the result in [43], the solution remains in  $\mathcal{R}_+^4$ . Further, adding the first three equations of the model (6), that is  $N_1 = S + V + I$ , and

$$\begin{aligned} D_t^\eta N_1 &= \Lambda - \kappa N_1 - \mu I, \\ &\leq \Lambda - \kappa N_1. \end{aligned} \quad (8)$$

Using the result given in [44], we get

$$N_1(t) \leq \frac{\Lambda}{\kappa} + \left( N_1(0) - \frac{\Lambda}{\kappa} \right) E_\eta(-\kappa t^\eta). \quad (9)$$

In (7),  $E_\eta$  is the Mittag-Leffler function. So, when  $t \rightarrow \infty$ , we get  $N_1(t) \rightarrow \Lambda/\kappa$ , and hence  $0 < N_1(t) \leq \Lambda/\kappa$ . Consider the last equation of the fractional system (6),

$$D_t^\eta E = \delta I - \beta E \leq \frac{\delta \Lambda}{\kappa} - \beta E, \quad (10)$$

it can be organized further as

$$D_t^\eta E + \beta E \leq \frac{\delta \Lambda}{\kappa}. \quad (11)$$

Using the result in [44], we obtain,

$$E(t) \leq \left( E(0) - \frac{\delta \Lambda}{\kappa} \right) E_\eta(-\beta t^\eta) + \frac{\delta \Lambda}{\beta \kappa},$$

when  $t \rightarrow \infty$ , then we have  $E(t) \rightarrow \delta \Lambda / \beta \kappa$ . Thus, all the solutions, starting in  $\mathcal{R}_+^4$  are restricted to the region  $\Omega_1 \times \Omega_2$ , where

$$\Omega_1 = \left\{ (S, V, I) \mid 0 \leq N_1 \leq \frac{\Lambda}{\kappa} \right\}, \text{ and } \Omega_2 = \left\{ E \mid 0 \leq E \leq \frac{\delta \Lambda}{\beta \kappa} \right\}. \quad (12)$$

□

We now provide the existence of a unique solution of the brucellosis model (6). We have the following result:

**Theorem 2** *A fractional brucellosis model (6) has a unique solution.*

**Proof** Consider  $K(t) = (S, V, I, E) = (k_1, k_2, k_3, k_4)^T$ , where  $T$  means transpose. Then the system (6) can be written in the matrix form as follows:

$$D_t^\eta K(t) = \mathcal{P}_1 K(t) + k_1 \mathcal{P}_2 K(t) + \mathcal{P}_3, \tag{13}$$

where the matrices  $\mathcal{P}_1, \mathcal{P}_2$ , and  $\mathcal{P}_3$  are defined as:

$$\mathcal{P}_1 = \begin{pmatrix} -\theta - \kappa & \omega & 0 & 0 \\ \theta & -\omega - \kappa & 0 & 0 \\ 0 & 0 & -\mu - \kappa & 0 \\ 0 & 0 & \delta & -\beta \end{pmatrix}, \quad \mathcal{P}_2 = \begin{pmatrix} 0 & 0 & -\frac{\tau_1}{N_1} & -\frac{\tau_2}{N_1} \\ 0 & 0 & 0 & 0 \\ 0 & 0 & \frac{\tau_1}{N_1} & \frac{\tau_2}{N_1} \\ 0 & 0 & 0 & 0 \end{pmatrix},$$

and

$$\mathcal{P}_3 = \begin{pmatrix} \Lambda \\ 0 \\ 0 \\ 0 \end{pmatrix}.$$

Denote  $\Phi(t, K(t)) = \mathcal{P}_1 K(t) + k_1 \mathcal{P}_2 K(t) + \mathcal{P}_3$ . We need to show that  $\Phi(t, K(t))$  satisfies the Lipschitz condition:

$$\begin{aligned} \|\Phi(t, K(t)) - \Phi(t, \bar{K}(t))\| &= \|\mathcal{P}_1 K(t) + k_1 \mathcal{P}_2 K(t) + \mathcal{P}_3 - (\mathcal{P}_1 \bar{K}(t) + k_1 \mathcal{P}_2 \bar{K}(t) + \mathcal{P}_3)\|, \\ &= \|(\mathcal{P}_1 + k_1 \mathcal{P}_2)(K(t) - \bar{K}(t))\|, \\ &\leq \mathcal{L} \|K(t) - \bar{K}(t)\|, \end{aligned}$$

where  $\mathcal{L} = \max(\mathcal{P}_1 + k_1 \mathcal{P}_2)$ , and  $\|\cdot\|$  is the usual Euclidean norm. Thus,  $\Phi(t, K(t))$  satisfy the Lipschitz condition. According to the theory of fractional differential equation from [45], the brucellosis system (6) has a unique solution. □

### 4 Equilibrium analysis

To obtain the disease-free equilibrium (DFE), we set the derivatives to zero and solve for  $S, V, I$ , and  $E$  when there is no infection in the population ( $I = 0$ , and  $E = 0$ ).  $D_t^\eta S = 0, D_t^\eta V = 0, D_t^\eta I = 0$ , and  $D_t^\eta E = 0$ . We have the DFE, denoted by  $\mathcal{L}_0$ , given by

$$\mathcal{L}_0 = (S^0, V^0, 0, 0) = \left( \frac{\Lambda(\kappa + \omega)}{\kappa(\theta + \kappa + \omega)}, \frac{\theta \Lambda}{\kappa(\theta + \kappa + \omega)}, 0, 0 \right). \tag{14}$$

#### 4.1 Basic reproduction number

The basic reproduction number  $\mathcal{R}_0$  can be derived using the next-generation matrix approach [46]:

$$F = \begin{pmatrix} \tau_1 \frac{S^0}{N_1^0} & \tau_2 \frac{S^0}{N_1^0} \\ 0 & 0 \end{pmatrix}, \text{ and } V = \begin{pmatrix} (\mu + \kappa) & 0 \\ -\delta & \beta \end{pmatrix}.$$

We have

$$\mathcal{R}_0 = \underbrace{\frac{\tau_1 S^0}{(\kappa + \mu) N_1^0}}_{\mathcal{R}_1} + \underbrace{\frac{\delta \tau_2 S^0}{\beta(\kappa + \mu) N_1^0}}_{\mathcal{R}_2}, \quad (15)$$

where  $N_1^0 = S^0 + V^0$ . The basic reproduction number can be defined as the average number secondary brucellosis infections generated by a single infected individual in a population that is completely vulnerable to brucellosis. It is useful in finding the stability of the model. If their value is less than unity then the model is locally or globally asymptotically stable, and hence the disease can be eliminated from the population while in the case it is greater than unity it might the disease spread in the community, and if it is equal one then the possibility of bifurcation can be exist of different types. We show the local asymptotical stability of the DFE  $\mathcal{L}_0$  in the following theorem.

**Theorem 3** *The brucellosis system at  $\mathcal{L}_0$  is locally asymptotically stable when  $\mathcal{R}_0 < 1$ .*

**Proof** At  $\mathcal{L}_0$ , we have the Jacobian matrix of the system (6)

$$J = \begin{pmatrix} -\theta - \kappa & \omega & -\frac{\tau_1 S^0}{N_1^0} & -\frac{\tau_2 S^0}{N_1^0} \\ \theta & -\kappa - \omega & 0 & 0 \\ 0 & 0 & -\kappa - \mu + \frac{\tau_1 S^0}{N_1^0} & \frac{\tau_2 S^0}{N_1^0} \\ 0 & 0 & \delta & -\beta \end{pmatrix}$$

Evaluating the matrix  $J$ , we obtain the following characteristic equation:

$$\lambda^4 + a_1 \lambda^3 + a_2 \lambda^2 + a_3 \lambda + a_4 = 0, \quad (16)$$

where

$$\begin{aligned} a_1 &= \beta + \theta + 2\kappa + \omega + (\kappa + \mu)(1 - \mathcal{R}_1), \\ a_2 &= \beta(\theta + 2\kappa + \omega) + \kappa(\theta + \kappa + \omega) + (\kappa + \mu)(\theta + 2\kappa + \omega)(1 - \mathcal{R}_1) \\ &\quad + \beta(\kappa + \mu)(1 - \mathcal{R}_0), \\ a_3 &= \beta\kappa(\theta + \kappa + \omega) + \kappa(\kappa + \mu)(\theta + \kappa + \omega)(1 - \mathcal{R}_1) \end{aligned}$$

$$\begin{aligned}
 & +\beta(\kappa + \mu)(\theta + 2\kappa + \omega)(1 - \mathcal{R}_0), \\
 a_4 & = \beta\kappa(\kappa + \mu)(\theta + \kappa + \omega)(1 - \mathcal{R}_0).
 \end{aligned}$$

The expressions for the coefficients  $a_1$  to  $a_4$  are given, and it's stated that these coefficients are positive when  $\mathcal{R}_0 < 1$  ( $\mathcal{R}_1 < \mathcal{R}_0$ ). Additionally, to ensure stability, the Routh-Hurwitz criterion  $a_k > 0, k = 1, \dots, 4$  and  $a_1a_2a_3 > a_3^2 + a_1^2a_4$  must be satisfied. Hence, the Routh-Hurwitz condition can be easily hold, and hence the model at  $\mathcal{L}$  is LAS when  $\mathcal{R}_0 < 1$ . □

Next, we present the global asymptotical stability of  $\mathcal{L}_0$ . First, we give the Lemma taken from [47].

**Lemma 1** *Assume that the function  $u(t) \in R^+$  is continuous and derivable, and then for every time  $t$ , we get  $t \geq t_0$ ,*

$$D_t^\eta \left( u(t) - u^*(t) - \ln \frac{u(t)}{u^*(t)} \right) \leq 1 - \frac{u^*(t)}{u(t)} D_t^\eta u(t), \quad u^* \in R^+, \quad \eta \in (0, 1). \quad (17)$$

**Theorem 4** *If  $\mathcal{R}_0 \leq 1$ , then, the DFE  $\mathcal{L}_0$  is GAS.*

**Proof** Let have the Lyapunov function  $L(t)$  as follows:

$$L(t) = \beta N_1^0 I + \tau_2 S^0 E. \quad (18)$$

Taking the fractional derivative of  $L(t)$  along the application of Lemma 1, we get

$$\begin{aligned}
 D_t^\eta L(t) & \leq \beta N_1^0 D_t^\eta I + \tau_2 S^0 D_t^\eta E, \\
 & = \beta N_1^0 \left[ \tau_1 \frac{SI}{N_1} + \tau_2 \frac{SE}{N_1} - \mu I - \kappa I \right] + \tau_2 S^0 [\delta I - \beta E], \\
 & = [\beta \tau_1 S^0 + \tau_2 S^0 \delta - (\mu + \kappa) \beta N_1^0] I + [\beta \tau_2 S^0 - \beta \tau_2 S^0] E, \\
 & = \beta N_1^0 (\mu + \kappa) (\mathcal{R}_0 - 1) I.
 \end{aligned} \quad (19)$$

Observe that  $D_t^\eta L(t) = 0$  at  $\mathcal{L}_0$ , and  $D_t^\eta L(t) \leq 0$  if  $\mathcal{R}_0 \leq 1$ . Thus, it follows from LaSalle Invariance principle that the DFE  $\mathcal{L}_0$  is GAS when  $\mathcal{R}_0 \leq 1$ . □

### 4.2 Endemic equilibria

The endemic equilibria of the model (6) denoted by  $\mathcal{L}_1 = (S^*, V^*, I^*, E^*)$ , and can be obtained when  $D_t^\eta S(t) = 0 \dots D_t^\eta E(t) = 0$ ,

$$S^* = \frac{\Lambda(\kappa + \omega)}{\theta\kappa + (\kappa + \Phi^*)(\kappa + \omega)}, \quad V^* = \frac{\theta\Lambda}{\theta\kappa + (\kappa + \Phi^*)(\kappa + \omega)}, \quad I^* = \frac{S^*\Phi^*}{\kappa + \mu}, \quad E^* = \frac{\delta I^*}{\beta}.$$

Inserting the above into

$$\Phi^* = \frac{(\tau_1 I^* + \tau_2 E^*) S^*}{N_1^*}, \quad (20)$$

where  $N_1^* = S^* + V^* + I^* + E^*$ , and simplifying, we get

$$a_0\Phi^* + a_1 = 0, \quad (21)$$

where

$$\begin{aligned} a_0 &= \beta(\kappa + \omega) + \delta(\kappa + \omega), \\ a_1 &= \beta(\kappa + \mu)(\theta + \kappa + \omega)(1 - \mathcal{R}_0). \end{aligned} \quad (22)$$

From (22),  $a_0 > 0$ , and  $a_1 > 0$  if  $\mathcal{R}_0 < 1$ . So,  $\Phi^* = -a_1/a_0$ , ensures that there exists a positive endemic equilibria when  $\mathcal{R}_0 > 1$ . Further, the linear expression of (21) suggests that there is no possibility of backward bifurcation in the brucellosis model (6).

## 5 Parameters estimation

Parameters estimations play an important role in disease epidemiology, as it helps in understanding the disease dynamics within populations. In epidemic systems, many parameters govern the disease spread and control, and accurate estimation of these parameters is essential for disease outcomes prediction, guiding public health interventions, and formulating control strategies. In this regard, here we consider the nonlinear least square technique by fitting the real cases of human brucellosis obtained from the source [48]. The number of cases considered per year. This method is useful and has been used in various fields and particularly in disease epidemiology for obtaining parameters estimations of a mathematical model. The goal of this technique is to determine the parameter values that minimize the sum of the squared differences between the predicted and actual data. The mathematical notation used is as follows:

$$\text{minimize } S(\psi) = \sum_{n=1}^k [z_n - l(t_n, \psi)]^2, \quad (23)$$

where  $z_n$  represents the actual real data of at time  $t_n$ ,  $l(t_n, \psi)$  is the system prediction value at  $t_n$  for the parameters set  $\psi$ , whereas  $S(\psi)$  is the sum of the squared of the given objective function. The brucellosis cases of humans obtained from the source [48] in mainland China for the period 2004 to 2018. From the given source, the annual cases reported in the mainland China in 2004 were 11472, so  $I_h(0) = 11472$ . The population of China in 2004 were 1.296 billion, so the population of healthy humans is  $S_h(0) = N_2(0) - I_h(0) = 1,296,800,000$ . The average life span in China as per the source in 2004 is  $\psi_h = \frac{1}{72.54}$  per year [49]. The birth can be calculated easily using the relation  $\Lambda_h \approx N_2(0) \times \psi_h$ . The rest of the parameters are fitted to the model versus data in the experiment.

The information about the number of sheep or its population is often difficult to find their exact value, however, a study about the recent information of sheep obtained from [50–52], that the initial value of  $S(0) = 5400000$ ,  $I(0) = 10000$ ,  $E(0) = 100000$ , and

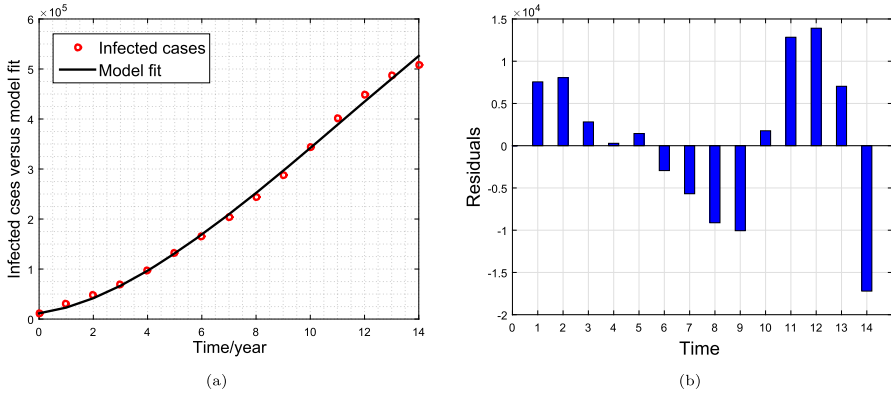


**Fig. 1** The plot describes the data fitting to the real cases of brucellosis: Sub-Figures (a) and (b) receptively represent the data fitting to the model and the corresponding residuals. In sub-Figures (a), the bold line indicates the model solution while the circle is the real data

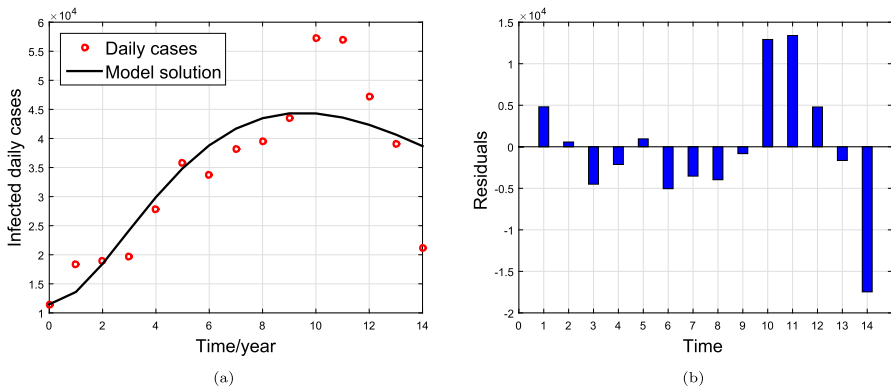


**Fig. 2** The plot shows the data fitting for the daily cases, and their corresponding residual, which are shown respectively in sub-figures (a) and (b)

$V(0) = 212912$  (but in our simulation, we consider the fitting without vaccination, and consider  $V(0) = 0$ ). The birth rate of livestock obtained from the source [50] is  $\Lambda = 2442000$ . The natural death rate is  $\kappa = 0.4514$  obtained from the expression  $\Lambda \approx \kappa \times N_1(0)$ . The remaining parameters given in the model (6) are fitted to the model and their values are given in Table 1.

To assess the quality of the fit, we calculated the Root Mean Square Error (RMSE) between the model predictions and the observed data. The RMSE is found to be 8424.6213, indicating a reasonable fit of the model to the data. Additionally the basic reproduction number,  $\mathcal{R}_0$ , which represents the average number of secondary infection produced by a single infected person in a fully susceptible population, was calculated as  $\mathcal{R}_0 = 1.0327$ . This value is slightly above 1 suggests that the infection has the potential to spread within the population, underscoring the importance of controlling measures. The fitting results are illustrated in Figs. 1, 2, and 3, where the model predictions (bold lines) are compared against the actual data (shown by circles) in Figs. 1a, and 2a. The

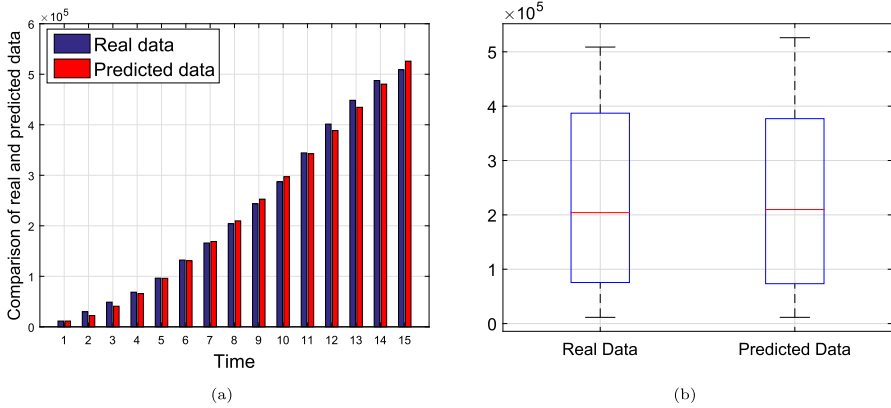


**Fig. 3** Comparison of real and predicted data through **a** bar graph and **b** box-plots

**Table 1** The parameters and their details obtained from experiments

Notation	Numerical value	Ref	Unit
$\tau_1$	0.4353	Fitted	Per contact
$\tau_2$	0.2754	Fitted	Per contact
$\mu$	0.0172	Fitted	day <sup>-1</sup>
$\delta$	0.0108	Fitted	day <sup>-1</sup>
$\beta$	0.0614	Fitted	day <sup>-1</sup>
$\phi_1$	0.3529	Fitted	day <sup>-1</sup>
$\phi_2$	0.0367	Fitted	day <sup>-1</sup>
$q$	0.0398	Fitted	day <sup>-1</sup>

residual plots highlight the difference among the model prediction and the real data, providing insight into the accuracy of the fit.

### 6 Numerical scheme

A numerical scheme to solve the system (3) constructed in Caputo derivative  $\alpha \in (0, 1]$  shall be presented. We will consider the Predictor-corrector method of Adams-Moulton type to get the numerical solution of the proposed fractional system, which was utilized in the literature [53, 54]. To derive the desired scheme, we need first to write the system (5) according to the following representation:

$$\begin{cases} {}^C D_t^\alpha \Phi(t) = \mathcal{M}(t, \Phi(t)) \\ \Phi(0) = \Phi_0, 0 < \mathcal{T} < \infty, \end{cases} \tag{24}$$

where  $\Phi = (S, V, I, E, S_h, I_h) \in \mathbb{R}^6$ ,  $\Phi_0$  is the initial value of the vector, and  $\mathcal{M}(t, \Phi(t))$  represents the continuous real-valued vector function that satisfies the Lipschitz condition. The application of the RL integral to system (24) both sides, we

have

$$\Phi(t) = \Phi_0 + \frac{1}{\Gamma(\eta)} \int_0^t (t - \chi)^\eta \mathcal{M}(\phi, \Phi(\phi)) d\phi. \tag{25}$$

Consider a uniform grid on the interval  $[0, T]$  with a step size defined as  $h = \frac{T-0}{m}$ ,  $m \in \mathbb{N}$ , where  $m$  represents a positive integer showing the number of sub-intervals in the given interval. It follows from the Euler method mentioned in [55], the equation (25) provides the following form:

$$\begin{cases} \Phi_{k+1} = \Phi_0 + \frac{h^\eta}{\Gamma(\eta+1)} \sum_{j=0}^k ((k - j + 1)^\eta - (k - j)^\eta) \mathcal{M}(t_j, \Phi(t_j)), \\ k = 0, 1, 2, \dots, m. \end{cases} \tag{26}$$

Utilizing equation (26) and by applying to the model (3), the following system is obtained:

$$\begin{aligned} S_{k+1} &= S_0 + L_1 \sum_{j=0}^k w_{k,j} [\Lambda - \tau_1 \frac{S_k I_k}{N_{1k}} - \tau_2 \frac{S_k E_k}{N_{1k}} - \theta S_k + \omega V_k - \kappa S_k], \\ V_{k+1} &= V_0 + L_1 \sum_{j=0}^k w_{k,j} (\theta S_k - \omega V_k - \kappa V_k), \\ I_{k+1} &= I_0 + L_1 \sum_{j=0}^k w_{k,j} \left( \tau_1 \frac{S_k I_k}{N_{1k}} + \tau_2 \frac{S_k E_k}{N_{1k}} - \mu I_k - \kappa I_k \right), \\ E_{k+1} &= E_0 + L_1 \sum_{j=0}^k w_{k,j} (\delta I_k - \beta E_k), \\ S_{k+1}^h &= S_0^h + L_1 \sum_{j=0}^k w_{k,j} \left( \Lambda_h - \phi_1 \frac{S_{hk} I_k}{N_{2k}} - \frac{\phi_2 S_{hk} E_k}{N_{2k}} - \psi_h S_{hk} + q I_{hk} \right), \\ I_{k+1}^h &= I_0^h + L_1 \sum_{j=0}^k w_{k,j} \left( \phi_1 \frac{S_{hk} I_k}{N_{2k}} + \frac{\phi_2 S_{hk} E_k}{N_{2k}} - \psi_h I_{hk} - q I_{hk} \right), \end{aligned} \tag{27}$$

where  $L_1 = \frac{h^\eta}{\Gamma(\eta+1)}$  and  $w_{k,j} = ((k - j + 1)^\eta - (k - j)^\eta)$ .

### 7 Numerical results

Here, we solve numerically the model (6) using the numerical values considered in Table 1. The numerical scheme presented in Sect. 6 is utilized to obtain the numerical results graphically in Figs. 4, 5, 6, 7, 8, 9 and 10. Figure 4 displays the influence of the memory index on the compartments of the system, susceptible, livestock, infected livestock, vaccinated livestock, brucellosis in the environment, susceptible and infected

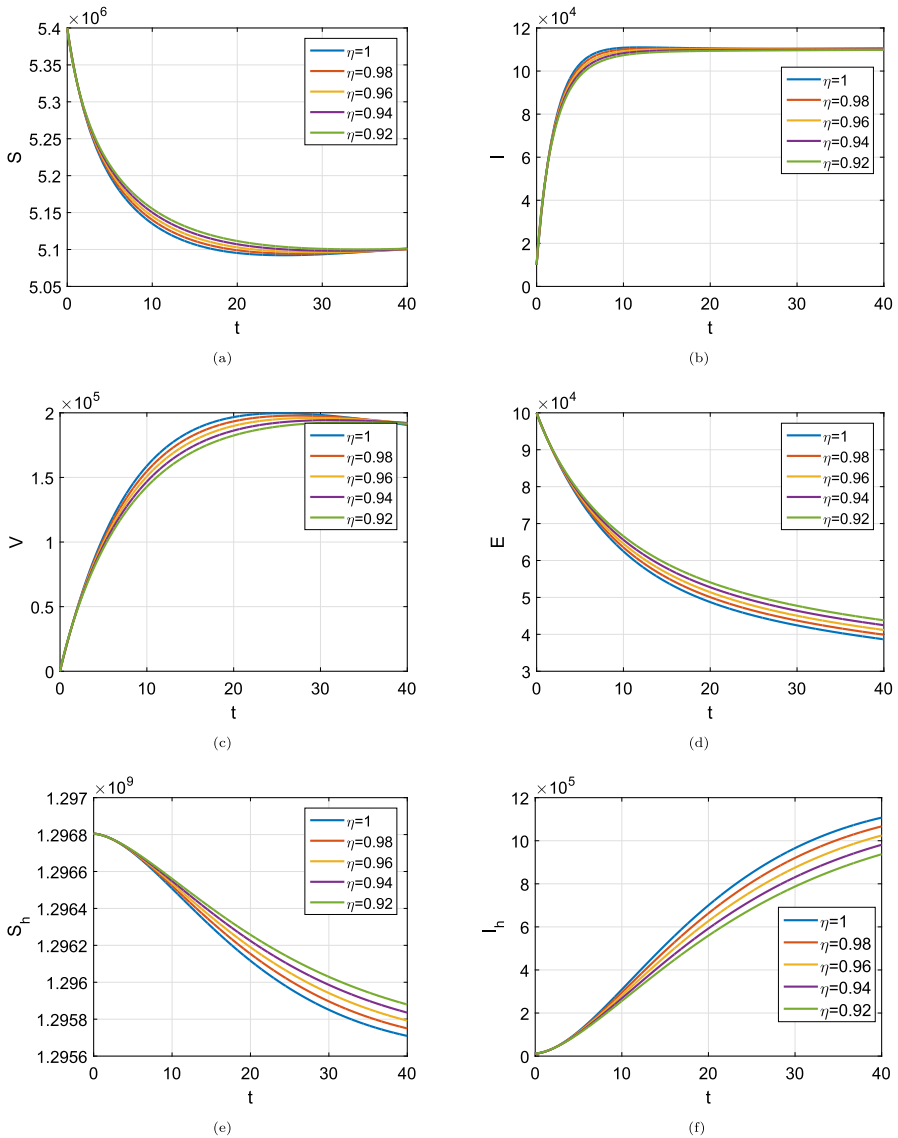


**Fig. 4** The plot shows the impact of the memory index on the model compartments,  $S$ ,  $I$ ,  $V$ ,  $E$ ,  $S_h$ , and  $I_h$  which are shown respectively in subfigures (a)–(f)

humans. From subfigures (a) to (f), one can observe that a higher memory index results in a slower initial response each compartment, suggesting that memory effects can delay the progression of the disease. Biologically, this aligns with the fact that historical exposures or immunity could affect current susceptibility and infection dynamics in both livestock and human population. The results are approaching to the equilibrium point which shows the importance of the proposed scheme.

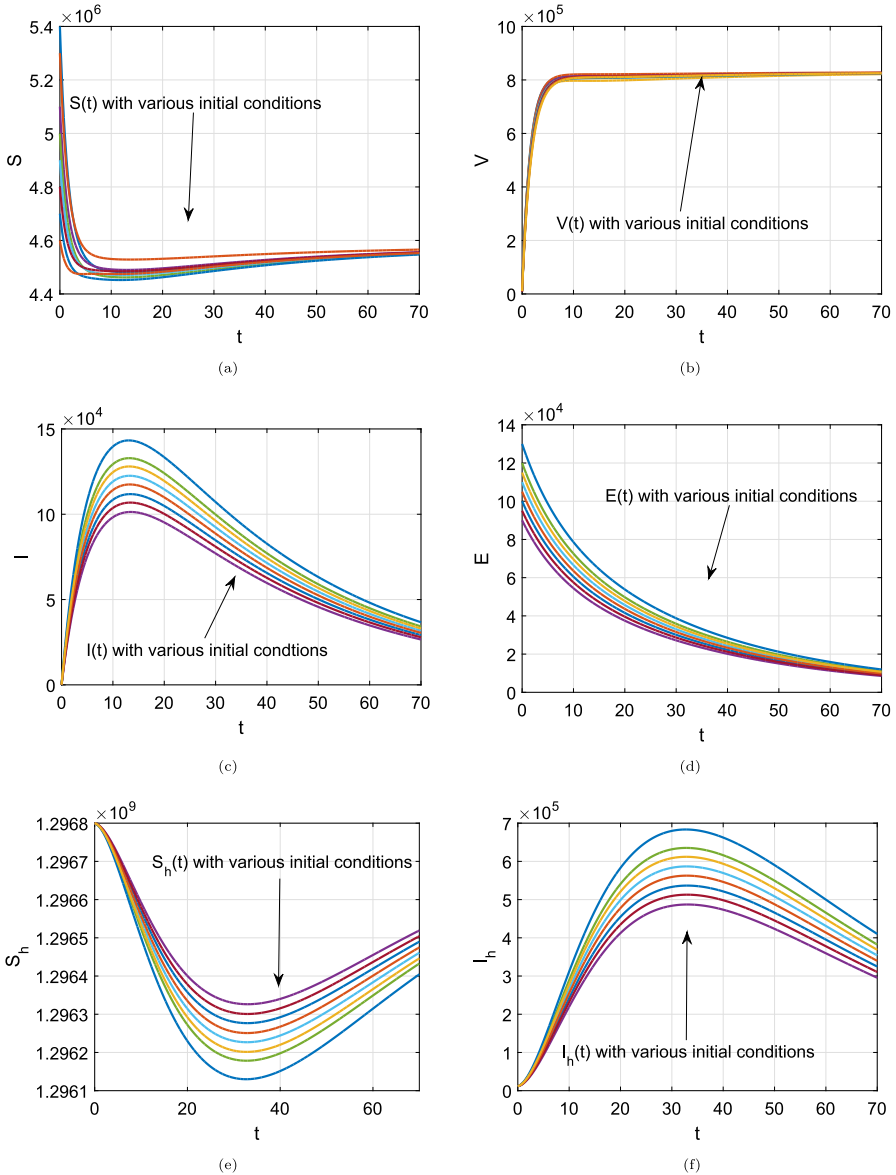


**Fig. 5** The plot shows the compartments of the model,  $S$ ,  $I$ ,  $V$ ,  $E$ ,  $S_h$ , and  $I_h$  with various initial conditions, respectively given in subfigures (a)–(f)

Figure 5 represents the compartments of the model under various initial conditions. It can be observed that with different initial conditions the model solution converges.

Figure 6 examines the impact of various values of  $\tau_1 = 0.4353, 0.3353, 0.2353$  on infected livestock, environmental brucellosis level and infected humans which are given respectively in (a)–(c). Lower values of  $\tau_1$  corresponds to a reduced transmission

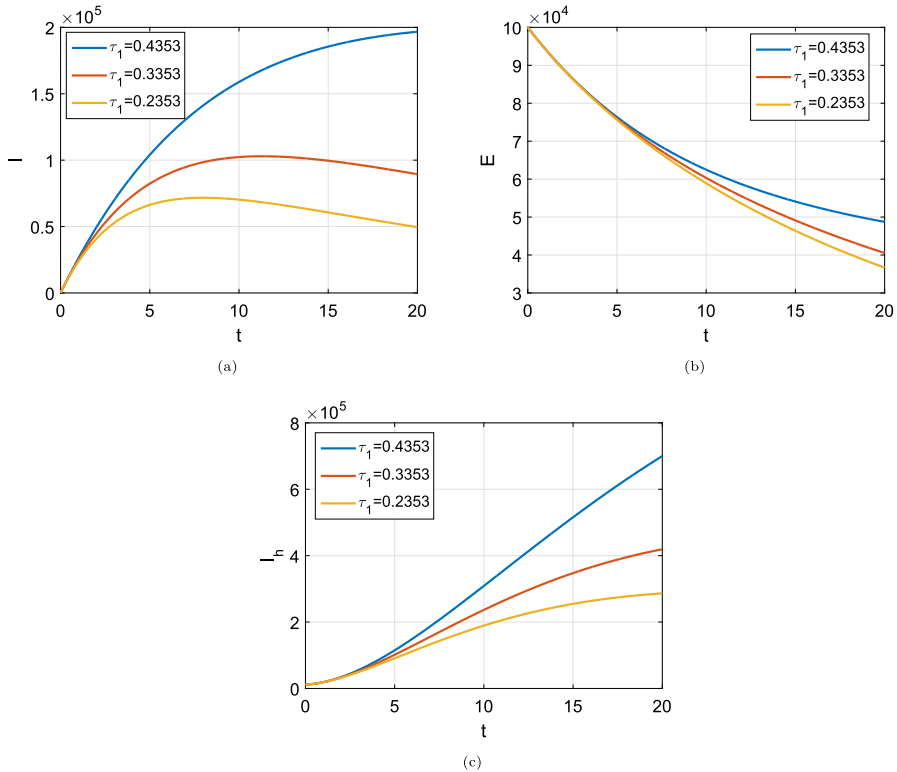


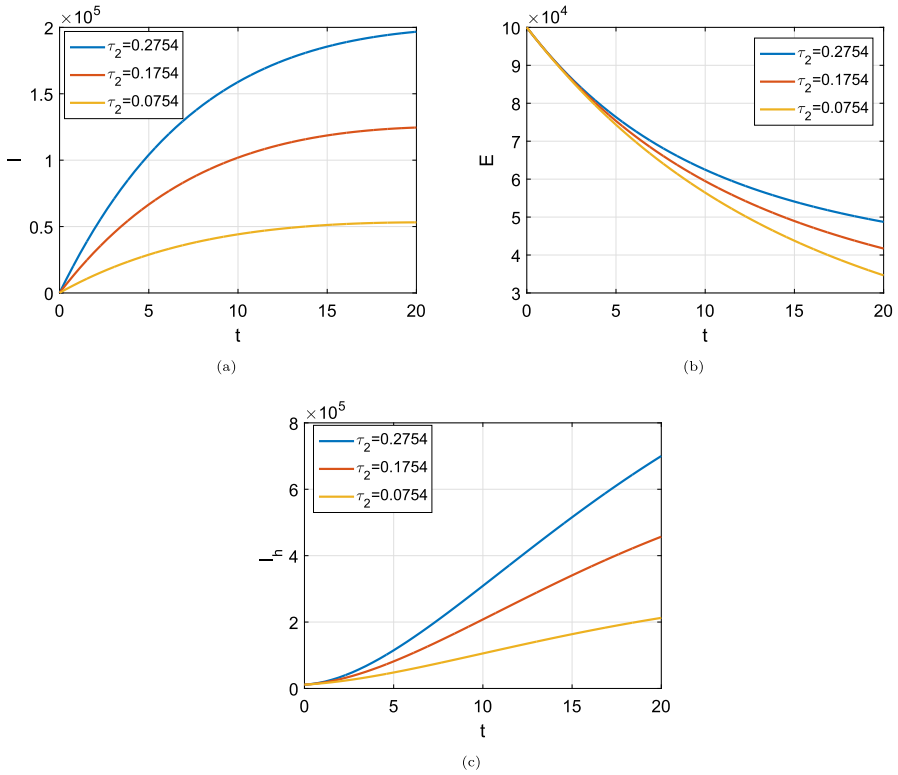
**Fig. 6** Figure shows the impact of  $\tau_1 = 0.4353, 0.3353, 0.2353$  on the infected classes of the model, where a–c are infected livestock, brucellosis in the environment, and the infected humans

rate from livestock to the environment, leading to lower environmental contamination. This, in turn, reduces the transmission to humans. The biological implication is that managing livestock infection levels can be an effective strategy for reducing overall disease burden in both the environment and the humans population.

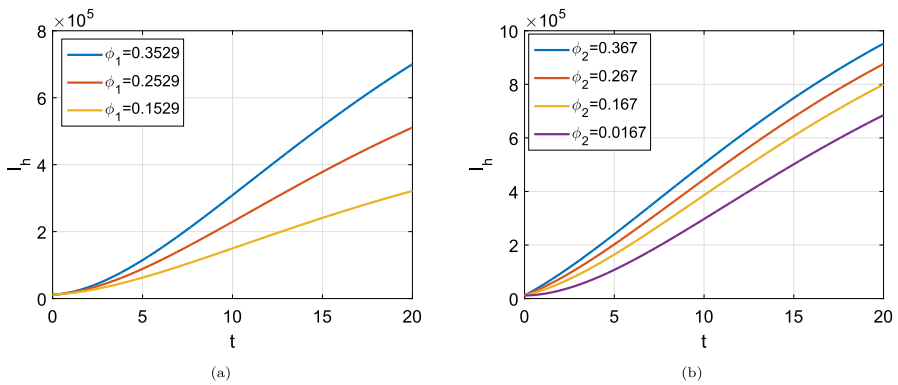
Figure 7 shows the influence of varying  $\tau_2 = 0.2754, 0.1754, 0.0754$  on the infected classes of the model. Subfigures a–c represent the infected livestock, environmental brucellosis, and infected humans, respectively. Decreasing  $\tau_2$  lead to a decrease in the infection spread from environment to livestock and humans, reducing brucellosis levels across all compartments. This indicates that controlling environmental contamination is crucial for reducing both humans and livestock infection rates.

Figure 8 demonstrates the effect of the transmission among humans, for the varying parameters  $\phi_1 = 0.3529, 0.2529, 0.1529$ , and  $\phi_2 = 0.367, 0.267, 0.167, 0.0167$  on humans infected people. Subfigure (a) examines the impact of varying  $\phi_1$ , while subfigure (b) explores  $\phi_2$ . As  $\phi_1$  and  $\phi_2$  decrease, the number of infected cases also decreases, emphasizing the significance of minimizing direct human transmission for effective disease control.

Figure 9 compares disease progression with and without vaccination, with parameters  $\theta = \omega = 0$  (no vaccine blue line) and  $\theta = 0.1, \omega = 0.01$  (with vaccine, red line).



**Fig. 7** Figure shows the impact of  $\tau_2 = 0.2754, 0.1754, 0.0754$  on the infected classes of the model, where **a–c** are infected livestock, brucellosis in the environment, and the infected humans



**Fig. 8** Figure shows the impact of  $\phi_1 = 0.3529, 0.2529, 0.1529$ , and  $\phi_2 = 0.367, 0.267, 0.167, 0.0167$  on the infected humans, where **a** is for the infected humans with varying  $\phi_1$  while **b** is for the infected humans with varying  $\phi_2$

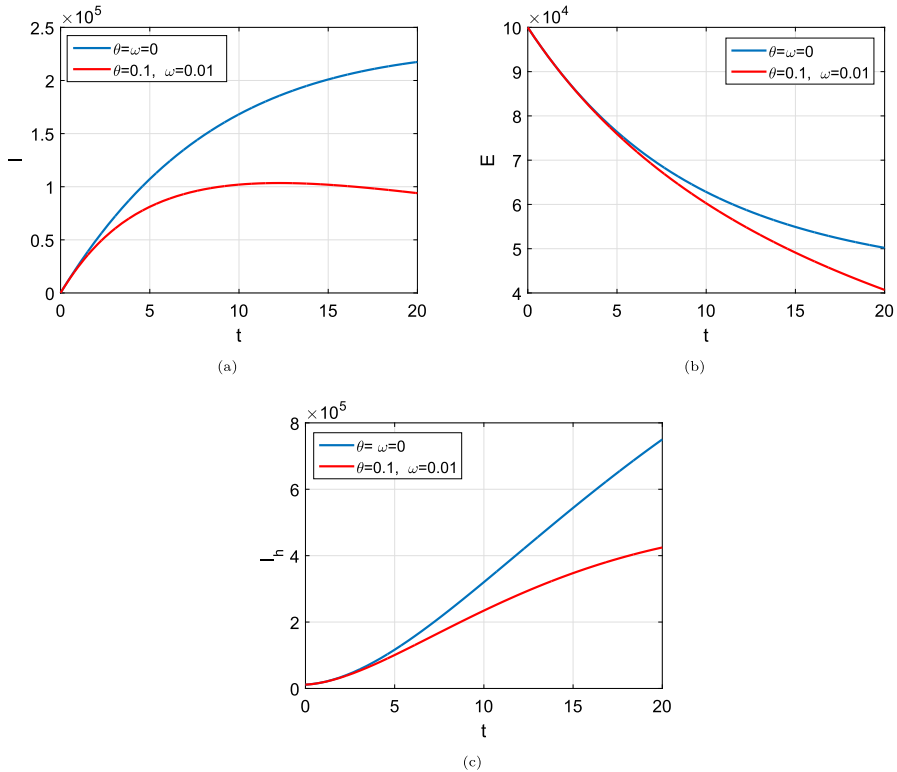


**Fig. 9** Figure shows the comparison of with vaccine ( $\theta = \omega = 0$ , bold blue line) and without vaccine ( $\theta = 0.1$ , and  $\omega = 0.01$ , bold red line). Subfigures a–c are the infected livestock, the amount of brucellosis in the environment, and the infected humans, respectively

Subfigures (a)–(c) show infected livestock, environmental brucellosis, and infected humans, respectively. Introducing vaccination significantly reduces infection levels in all compartments, particularly among the humans. This highlights the effectiveness of vaccination in controlling brucellosis spread through direct and environmental transmission routes.

Figure 10 investigates the impact of varying the vaccination parameter  $\theta = 0.01, 0.1, 0.2, 0.3$ , and  $\omega = 0.01$  held constant, on infected livestock, environmental brucellosis, and infected humans, respectively in (a)–(c). Higher vaccination rate lead to a notable reduction in infection prevalences across all compartments, reinforcing the role of widespread vaccination coverage in reducing brucellosis transmission and infection in both livestock and humans.

## 8 Conclusion

In this study, we developed and analyzed a mathematical model to describe the transmission dynamics of brucellosis in humans and animals, incorporating key factors

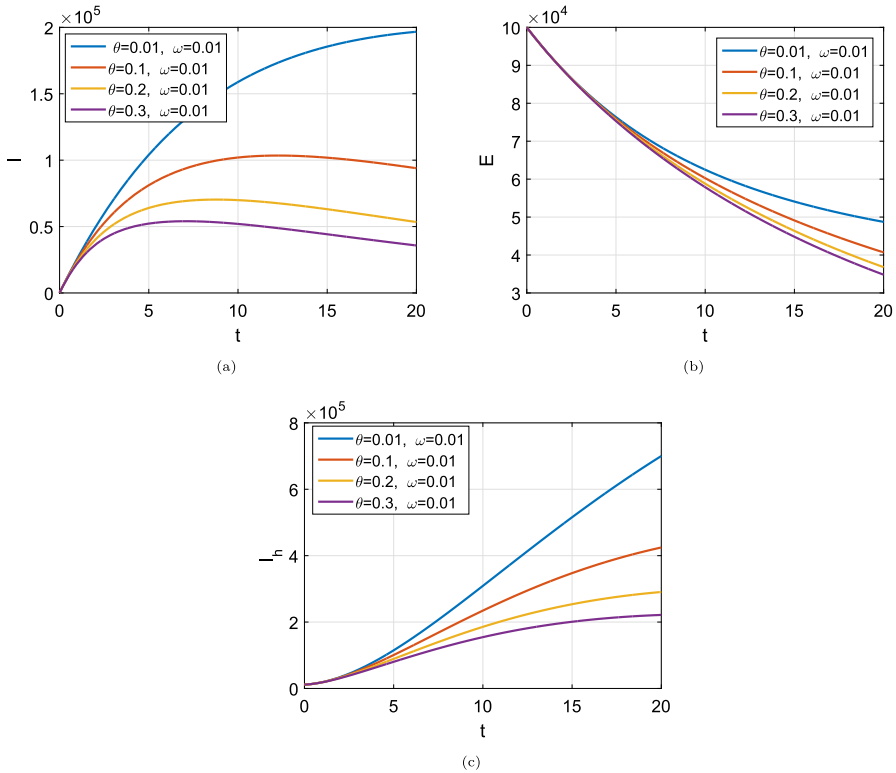


**Fig. 10** Figure shows the comparison impact on the infected compartments of the model when varying  $\theta = 0.01, 0.1, 0.2, 0.3$ , and  $\omega = 0.01$  (fixed). Subfigures **a–c** are the infected livestock, the amount of brucellosis in the environment, and the infected humans, respectively

such as infection, recovery, environmental transmission, vaccination etc. The model is extended to fractional system using Caputo derivative from the integer order model. The existence of the fractional system and their respective results are obtained. By establishing the basic reproduction number  $\mathcal{R}_0$ , we demonstrated that the DFE is locally asymptotically stable when  $\mathcal{R}_0 < 1$ , implying that brucellosis can be eradicated if  $\mathcal{R}_0$  is maintained below this threshold. For  $\mathcal{R}_0 \leq 1$ , we proved the global asymptotic stability of the DFE. For endemic equilibria, we showed that a positive endemic equilibrium exists when  $\mathcal{R}_0 > 1$ , indicating persistence disease presence. Importantly, our analysis of the endemic equilibrium revealed no possibility of backward bifurcation, suggesting that reducing  $\mathcal{R}_0$  below one is sufficient to prevent disease persistence without the risk of sudden resurgence.

To further validate our model, we applied the nonlinear least squares method to fit the model human brucellosis data from mainland China (2004–2018). With the help of the parameters, the numerical value computed for  $\mathcal{R}_0 = 1.0327$ . This parameter estimation provided insights into the model’s accuracy and its potential for guiding intervention strategies. Overall, this work underscores the importance of controlling  $\mathcal{R}_0$  in managing outbreaks. It highlights that maintaining  $\mathcal{R}_0 < 1$  through effective

control measures, such as vaccination, and improved bio-security, can lead to disease elimination. Future research can build upon this model by including additional factors such as seasonal transmission, spatial distribution, or host specific behaviors, further enhancing the model's applicability in diverse epidemiological settings.

**Acknowledgements** The authors are thankful to the Deanship of Research and Graduate Studies, King Khalid University, Abha, Saudi Arabia, for financially supporting this work through the Large Research Group Project under Grant no. R.G.P.2/517/45.

**Author contributions** All authors equally contributed in this work.

**Funding** Open access funding provided by University of the Free State.

**Data availability** The data is available from the corresponding author on a reasonable request.

## Declarations

**Conflict of interest** No potential Conflict of interest exists regarding this publication.

**Open Access** This article is licensed under a Creative Commons Attribution 4.0 International License, which permits use, sharing, adaptation, distribution and reproduction in any medium or format, as long as you give appropriate credit to the original author(s) and the source, provide a link to the Creative Commons licence, and indicate if changes were made. The images or other third party material in this article are included in the article's Creative Commons licence, unless indicated otherwise in a credit line to the material. If material is not included in the article's Creative Commons licence and your intended use is not permitted by statutory regulation or exceeds the permitted use, you will need to obtain permission directly from the copyright holder. To view a copy of this licence, visit <http://creativecommons.org/licenses/by/4.0/>.

## References

1. Lai, S., Chen, Q., Li, Z.: Human brucellosis: an ongoing global health challenge. *China CDC Weekly* **3**(6), 120 (2021)
2. McDermott, J., Grace, D., Zinsstag, J.: Economics of brucellosis impact and control in low-income countries. *Revue Sci. Tech. (Int. Off. Epizoot.)* **32**(1), 249–261 (2013)
3. Yang, H., Zhang, G., Luo, P., He, Z., Hu, F., Li, L., Allain, J.-P., Li, C., Wang, W.: Detection of brucellae in peripheral blood mononuclear cells for monitoring therapeutic efficacy of brucellosis infection. *Antimicrob. Resist. Infect. Control* **8**, 1–9 (2019)
4. Wang, Y., Xu, C., Zhang, S., Wang, Z., Zhu, Y., Yuan, J.: Temporal trends analysis of human brucellosis incidence in mainland china from 2004 to 2018. *Sci. Rep.* **8**(1), 15901 (2018)
5. Zhao, C., Yang, Y., Wu, S., Wu, W., Xue, H., An, K., Zhen, Q.: Search trends and prediction of human brucellosis using Baidu index data from 2011 to 2018 in China. *Sci. Rep.* **10**(1), 5896 (2020)
6. Hill, E.M., Prosser, N.S., Ferguson, E., Kaler, J., Green, M.J., Keeling, M.J., Tildesley, M.J.: Modelling livestock infectious disease control policy under differing social perspectives on vaccination behaviour. *PLoS Comput. Biol.* **18**(7), 1010235 (2022)
7. Sun, X., Wang, G.: Changes of mutton price in Shaanxi province and its influence on farmers. *Heilongjiang Anim. Husb. Vet* **10**, 5–7 (2017)
8. Shone, R.: *An Introduction to Economic Dynamics*. Cambridge University Press, Cambridge (2001)
9. Sun, G.Q., Zhang, H.T., Chang, L.L., Jin, Z., Wang, H., Ruan, S.G.: On the dynamics of a diffusive foot-and-mouth disease model with nonlocal infections. *SIAM J. Appl. Math.* **82**(4), 1587–1610 (2022)
10. Ma, X., Luo, X.F., Li, L., Li, Y., Sun, G.Q.: The influence of mask use on the spread of covid-19 during pandemic in New York city. *Results Phys.* **34**, 105224 (2022). <https://doi.org/10.1016/j.rinp.2022.105224>
11. Bajiya, V.P., Tripathi, J.P., Kakkar, V., Wang, J., Sun, G.Q.: Global dynamics of a multi-group seir epidemic model with infection age. *Chin. Ann. Math. Ser. B* **42**(6), 833–860 (2021)

12. Ainseba, B.E., Benosman, C., Magal, P.: A model for ovine brucellosis incorporating direct and indirect transmission. *J. Biol. Dyn.* **4**, 2–11 (2010)
13. Li, M.T., Sun, G.Q., Zhang, J., Jin, Z., Sun, X.D., Wang, Y.M., et al.: Transmission dynamics and control for a brucellosis model in hinggan league of inner Mongolia, China. *Math. Biosci. Eng.* **11**, 1115–1137 (2014)
14. Kenne, C., Mophou, G., Dorville, R., Zongo, P.: A model for brucellosis disease incorporating age of infection and waning immunity. *Mathematics* **10**(4), 670 (2022)
15. Nie, J., Sun, G.Q., Sun, X.D., Zhang, J., Wang, N., Wang, Y.M., et al.: Modeling the transmission dynamics of dairy cattle brucellosis in Jilin Province, China. *J. Biol. Syst.* **22**, 533–554 (2014)
16. Zhang, J., Jin, Z.: The application of the nonautonomous dynamics model on brucellosis in hinggan league. *J. Inner Mongolia Normal Univ. (Nat. Sci. Ed.)* **44**, 1–4 (2015)
17. Zhang, J., Jin, Z., Li, L., Sun, X.D.: Cost assessment of control measure for brucellosis in Jilin Province, China. *Chaos Solitons Fractals* **104**, 798–805 (2017)
18. Li, M.T., Pei, X., Zhang, J., Li, L.: Asymptotic analysis of endemic equilibrium to a brucellosis model. *Math. Biosci. Eng.* **16**, 5836–5850 (2019)
19. Li, M.T., Sun, G.Q., Jin, Z.: Dynamic analysis of sheep brucellosis with stage structure. In: Highlights of Sciencepaper Online, vol. 7, pp. 53–57. (2014)
20. Hou, Q., Sun, X.D.: Modeling sheep brucellosis transmission with a multi-stage model in Changling County of Jilin Province, China. *J. Appl. Math. Comput.* **51**, 227–244 (2016)
21. Beauvais, W., Musallam, I., Guitian, J.: Vaccination control programs for multiple livestock host species: an age-stratified, seasonal transmission model for brucellosis control in endemic settings. *Parasites Vectors* **9**, 55 (2016)
22. Hou, Q., Sun, X.D., Zhang, J., Liu, Y., Jin, Z.: Modeling the transmission dynamics of sheep brucellosis in inner Mongolia Autonomous Region, China. *Math. Biosci.* **242**, 51–58 (2013)
23. Li, M.T., Sun, G.Q., Wu, Y.F., Zhang, J., Jin, Z.: Transmission dynamics of a multi-group brucellosis model with mixed cross infection in public farm. *Appl. Math. Comput.* **234**, 582–594 (2014)
24. Li, M.T., Jin, Z., Sun, G.Q., Zhang, J.: Modeling direct and indirect disease transmission using multi-group model. *J. Math. Anal. Appl.* **446**, 1292–1309 (2017)
25. Sabir, Z., Raja, M., Alhazmi, S.E., Gupta, M., Arbi, A., Baba, I.A.: Applications of artificial neural network to solve the nonlinear covid-19 mathematical model based on the dynamics of siq. *J. Taibah Univ. Sci.* **16**(1), 874–884 (2022)
26. Sabir, Z., Hashem, A.F., Arbi, A., Abdelkawy, M.A.: Designing a Bayesian regularization approach to solve the fractional Layla and Majnun system. *Mathematics* **11**(17), 3792 (2023)
27. Sabir, Z., Mehmood, M.A., Umar, M., Salahshour, S., Altun, Y., Arbi, A., Ali, M.R.: A numerical treatment through Bayesian regularization neural network for the chickenpox disease model. *Comput. Biol. Med.* **187**, 109807 (2025)
28. Kumar, S., Chauhan, R.P., Momani, S., Hadid, S.: Numerical investigations on covid-19 model through singular and non-singular fractional operators. *Numer. Methods Part. Differ. Eq.* **40**(1), 22707 (2024)
29. Logeswari, K., Ravichandran, C., Nisar, K.S.: Mathematical model for spreading of covid-19 virus with the Mittag-Leffler kernel. *Numer. Methods Part. Differ. Eq.* **40**(1), 22652 (2024)
30. Zafar, Z.U.A., Khan, M.A., Akgül, A., Asiri, M., Riaz, M.B.: The analysis of a new fractional model to the zika virus infection with mutant. *Heliyon* **10**(1) (2024)
31. Shah, K., Khan, A., Abdalla, B., Abdeljawad, T., Khan, K.A.: A mathematical model for nipah virus disease by using piecewise fractional order caputo derivative. *Fractals*, 2440013 (2024)
32. Srilekha, R., Parthiban, V.: Simulink methods to simulate covid-19 outbreak using fractional order models. *Contemporary Mathematics*, pp. 157–174 (2024)
33. Babakordi, F., Allahviranloo, T.: Application of fuzzy abc fractional differential equations in infectious diseases. *Comput. Methods Differ. Eq.* **12**(1), 1–15 (2024)
34. Arbi, A.: Robust model predictive control for fractional-order descriptor systems with uncertainty. *Fract. Calculus Appl. Anal.* **27**(1), 173–189 (2024)
35. Bhattar, S., Jangid, K., Abidemi, A., Owolabi, K.M., Purohit, S.D., et al.: A new fractional mathematical model to study the impact of vaccination on covid-19 outbreaks. *Decis. Anal. J.* **6**, 10015 (2023)
36. Abbes, A., Ouannas, A., Shawagfeh, N., Jahanshahi, H.: The fractional-order discrete covid-19 pandemic model: stability and chaos. *Nonlinear Dyn.* **111**(1), 965–983 (2023)
37. Shutaywi, M., Shah, Z., Vrinceanu, N., Jan, R., Deebani, W.: Exploring the dynamics of hiv and cd4+ t-cells with non-integer derivatives involving nonsingular and nonlocal kernel. *Sci. Rep.* **14**(1), 24506 (2024)

38. Alshehri, A., Shah, Z., Jan, R.: Mathematical study of the dynamics of lymphatic filariasis infection via fractional-calculus. *Eur. Phys. J. Plus* **138**(3), 1–15 (2023)
39. Farhan, M., Shah, Z., Jan, R., Islam, S.: A fractional modeling approach of buruli ulcer in possum mammals. *Phys. Scr.* **98**(6), 065219 (2023)
40. Tang, T.-Q., Rehman, Z.U., Shah, Z., Jan, R., Vrinceanu, N., Racheriu, M.: Modeling and analysis of the transmission of avian spirochetosis with non-singular and non-local kernel. *Comput. Methods Biomech. Biomed. Engin.* **27**(7), 905–917 (2024)
41. Podlubny, I.: *Fractional Differential Equations: An Introduction to Fractional Derivatives, Fractional Differential Equations, to Methods of Their Solution and Some of Their Applications*. Elsevier, Amsterdam (1998)
42. Almeida, R., Cruz, A.M., Martins, N., Monteiro, M.: An epidemiological mseir model described by the caputo fractional derivative. *Int. J. Dyn. Control* **7**, 776–784 (2019)
43. Odibat, Z.M., Shawagfeh, N.T.: Generalized taylor's formula. *Appl. Math. Comput.* **186**(1), 286–293 (2007)
44. Li, H.-L., Zhang, L., Hu, C., Jiang, Y.-L., Teng, Z.: Dynamical analysis of a fractional-order predator-prey model incorporating a prey refuge. *J. Appl. Math. Comput.* **54**, 435–449 (2017)
45. Diethelm, K., Ford, N.J.: Analysis of fractional differential equations. *J. Math. Anal. Appl.* **265**(2), 229–248 (2002)
46. Driessche, P., Watmough, J.: Reproduction numbers and sub-threshold endemic equilibria for compartmental models of disease transmission. *Math. Biosci.* **180**(1–2), 29–48 (2002)
47. Vargas-De-León, C.: Volterra-type lyapunov functions for fractional-order epidemic systems. *Commun. Nonlinear Sci. Numer. Simul.* **24**(1–3), 75–85 (2015)
48. Sun, G.-Q., Li, M.-T., Zhang, J., Zhang, W., Pei, X., Jin, Z.: Transmission dynamics of brucellosis: mathematical modelling and applications in china. *Comput. Struct. Biotechnol. J.* **18**, 3843–3860 (2020)
49. China Life Expectancy 1950-2024, <https://www.macrotrends.net/global-metrics/countries/CHN/china/life-expectancy>, Accessed on August 24, 2024
50. NBSRPC. China statistical yearbook-2021. China Statistics Press. Accessed on 24 August 2024 (2021)
51. NDRC. Compilation of cost-benefit data of national agricultural products. China Statistics Press. Accessed on 24 August 2024 (2021)
52. Wang, L.-S., Li, M.-T., Pei, X., Zhang, J., Sun, G.-Q., Jin, Z.: Cost assessment of optimal control strategy for brucellosis dynamic model based on economic factors. *Commun. Nonlinear Sci. Numer. Simul.* **124**, 107310 (2023)
53. Jajarmi, A., Baleanu, D.: A new fractional analysis on the interaction of HIV with cd4+ t-cells. *Chaos Solitons Fractals* **113**, 221–229 (2018)
54. Sun, T.-C., DarAssi, M.H., Alfwzan, W.F., Khan, M.A., Alqahtani, A.S., Alshahrani, S.S., Muhammad, T.: Mathematical modeling of covid-19 with vaccination using fractional derivative: a case study. *Fractal Fract.* **7**(3), 234 (2023)
55. Li, C., Zeng, F.: *Numerical Methods for Fractional Calculus*. CRC Press, Boca Raton (2015)

**Publisher's Note** Springer Nature remains neutral with regard to jurisdictional claims in published maps and institutional affiliations.